

## SUN LOAD ANALYSIS AND TESTING ON AUTOMOTIVE FRONT LIGHTING PRODUCTS

Emre Öztürk, Mehmet Aktaş, and Tunç Şenyüz

*Magneti Marelli Mako Elektrik Sanayi Ve Ticaret A.Ş., Bursa, Turkey*  
E-mails: [emre.ozturk@magnetimarelli.com](mailto:emre.ozturk@magnetimarelli.com); [mehmet.aktas@magnetimarelli.com](mailto:mehmet.aktas@magnetimarelli.com);  
[tunc.senyuz@magnetimarelli.com](mailto:tunc.senyuz@magnetimarelli.com)

---

### ABSTRACT

The purpose of this research is to reach good correlation between sun load simulation and solar focusing test for exterior automotive lighting products. Light coming from sun is highly collimated (parallel rays) and focusable from lenses with concave structure. Focusing incidence leads to a hot spot on lens surrounding plastic parts which may cause melting failures at high temperature zones. Sun load simulation is performing to eliminate risk of discoloration, deformation, out gassing, coating failures and fire with prolonged exposure from field. Irradiance values in  $W/m^2$  defined in simulation as heat source depending of an angle of incidence of the sun radiation. At first step, simulation is performing with 5 degree intervals to define the critical zones then intervals decreased to 2 degree to detect the critical azimuth and inclination angles. Critical azimuth and inclination angles is checking with ray trace analysis to check the bouncing of sun rays and possible solution to eliminate focuses with design solutions. After numerical analysis to release and validate the automotive lighting products regarding the sun load test, measurement with first parts is necessary. Measurement is performing for all critical angles which have been detected at simulation with thermal camera under ultra high-collimation solar simulator. Measured temperatures are settled according to environment conditions and correlation is checking with simulations.

**Keywords:** sun load, automotive lighting, hot spot, burning glass, Computational Fluid Dynamics (CFD) Thermal Analysis

### 1. INTRODUCTION

Sunlight is known to melt materials in the case of focusing. Sunlight damage experiments were carried out with the help of a simple magnifying glass and results described as a burning glass effect. Unlike other light sources, the sun rays can be highly focused by the lenses due to the parallelism (Fig. 1.a) [1]. In parallel with the increase number of lenses and plastic materials usage in automotive sector, many new types of burning glass fault type have begun to be observed. The light emitting diode (LED) and high-intensity discharge (HID) bulbs, which are used in the application of high-tech automotive lighting products, require the use of short focal points in terms of appropriate light distribution [2,3]. This necessity causes unwanted focuses on the plastic aesthetic parts, which are used around the lenses. As a result of these focuses, discoloration, deformation, out gassing, and burns occur as a consequence of long-term loads on the parts.

Depending on the angles of the incoming rays, the focuses may occur on the front or back of the lenses (Fig 1.b). For this reason, the lenses used in automotive lighting products must be checked against the effects of sun load.

### 2. MATERIAL AND METHOD

In the studies, different types of the projectors (Fig. 2) and shell reflector (Fig. 3), which are frequently used to hide the light source in the new lighting products, have been examined.

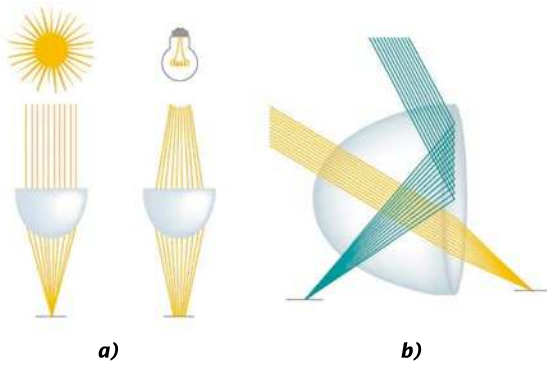


Fig. 1. Sunlight focusing (a) & front and rear surface focusing (b)

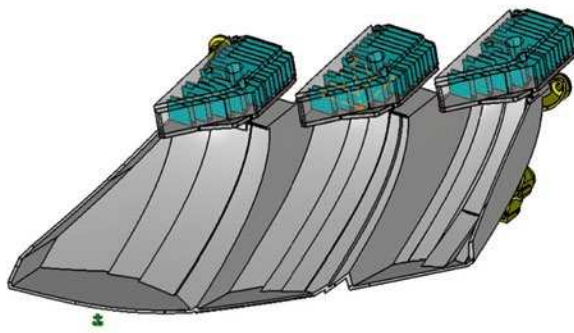


Fig 3. Shell Reflector

The focuses may occur on the aesthetic parts around the projector lenses or shell reflectors. The focusing point varies depending on the interior design of the lighting product and the part characteristics (coating, surface angles, etc.).

At the first step lighting project work shown in Fig. 4, cover panel, tubus and HID frame has been examined without aluminium coating and raw materials are chosen as black. In the front lighting project work shown in Fig. 5, the black separator part has been examined which is designed aesthetically to cover shell reflector.

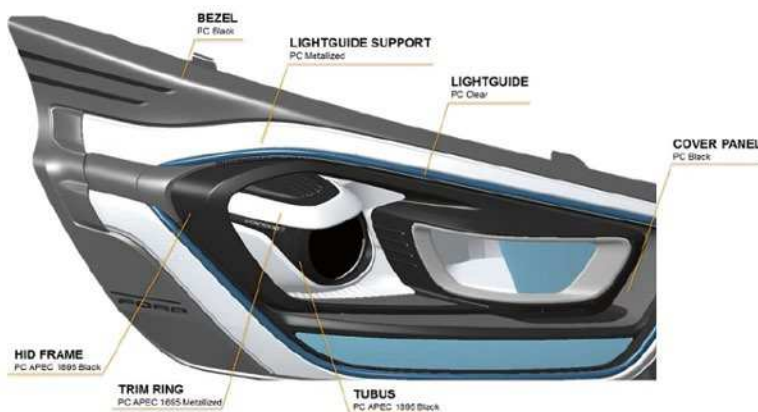


Fig 4. Project study with projector



Fig 2. Projector types

In accordance with the requirements of the parts requested by the customer, components have been identified that may pose a risk when subjected to the sun load in design reviews. In the first place thermal analysis; critical angle definition, ray trace analysis carried out respectively, which is followed by the final thermal simulation with the change of temperature to control the maximum operating conditions. The critical angles determined in the analysis results have been tested by the established mechanism and correlation between analysis and test has been performed.

### 2.1. Theoretical study

Direct solar radiation (assuming fresh air) based on the theory of optical air mass (AM) has been defined.

$$E_{direct} = E_0 \cdot 0.76^{AM^{0.618}}, \quad (1)$$

where  $E_0 = 1353 \text{ W/m}^2$  is the solar constant,  $AM \geq \sim 0.5$  is the optical air mass.

The air mass, which is based on Kasten and Young [4], depends on a height of  $h$  above sea level and the zenith angle of  $\gamma$  with earth radius equal to 6378 km and  $h_{atm} = 8.7 \text{ km}$

The latitude has been taken as  $0^\circ$  (21 March or 21 September) and the zenith angle has been accept-

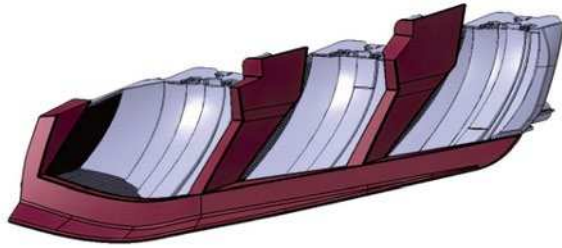


Fig 5. Project study with the shell reflector

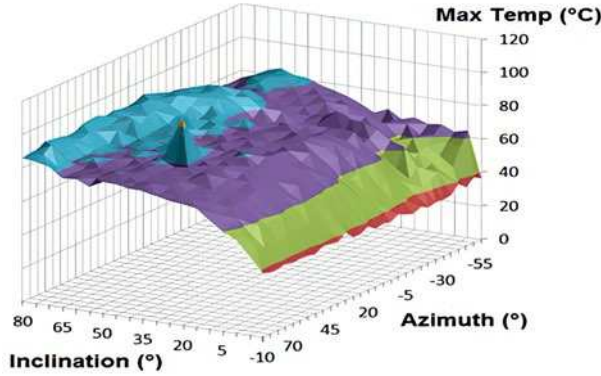


Fig. 6. The 5 degrees angles scan results

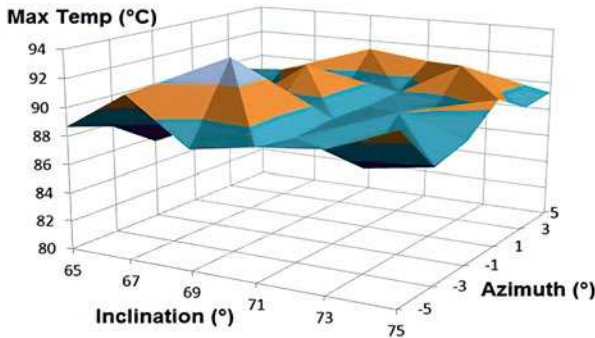


Fig. 7. The 2 degrees angles scan results

ed at 0° – 90°. The devices used in solar load measurements have been placed at a height of  $h = 2$  km above sea level and calculated based on the data at this height. Depending on the angle, the radiation values have been calculated and used as input for thermal analysis.

The numerical simulation was performed under steady-state conditions and the air flow was assumed as laminar. The numerical solution includes all heat transfer nodes. The governing equations including continuity, momentum, and energy equations for steady-state conditions of air flow with free convection effects can be written by using equations (3–7). The equation 8 is solved numerically for solid regions without heat generation. The related equations cannot be compressed in the Cartesian coordinate system and can be written by us-

ing the Boussinesq approach for steady-state flow as follows:

$$\frac{\partial u}{\partial x} + \frac{\partial v}{\partial y} + \frac{\partial w}{\partial z} = 0, \quad (2)$$

$$u \cdot \frac{\partial u}{\partial x} + v \cdot \frac{\partial u}{\partial y} + w \cdot \frac{\partial u}{\partial z} = -\frac{1}{\rho} \cdot \frac{\partial p}{\partial x} + v \left( \frac{\partial^2 u}{\partial x^2} + \frac{\partial^2 u}{\partial y^2} + \frac{\partial^2 u}{\partial z^2} \right), \quad (3)$$

$$u \cdot \frac{\partial v}{\partial x} + v \cdot \frac{\partial v}{\partial y} + w \cdot \frac{\partial v}{\partial z} = -\frac{1}{\rho} \cdot \frac{\partial p}{\partial y} + v \cdot \left( \frac{\partial^2 v}{\partial x^2} + \frac{\partial^2 v}{\partial y^2} + \frac{\partial^2 v}{\partial z^2} \right), \quad (4)$$

$$u \cdot \frac{\partial w}{\partial x} + v \cdot \frac{\partial w}{\partial y} + w \cdot \frac{\partial w}{\partial z} = -\frac{1}{\rho} \cdot \frac{\partial p}{\partial z} + v \left( \frac{\partial^2 w}{\partial x^2} + \frac{\partial^2 w}{\partial y^2} + \frac{\partial^2 w}{\partial z^2} \right) + g\beta(T - T_\infty), \quad (5)$$

$$u \cdot \frac{\partial T}{\partial x} + v \cdot \frac{\partial T}{\partial y} + w \cdot \frac{\partial T}{\partial z} = \alpha \cdot \left( \frac{\partial^2 T}{\partial x^2} + \frac{\partial^2 T}{\partial y^2} + \frac{\partial^2 T}{\partial z^2} \right), \quad (6)$$

$$\frac{\partial^2 T}{\partial x^2} + \frac{\partial^2 T}{\partial y^2} + \frac{\partial^2 T}{\partial z^2} + \frac{q}{k} = 0, \quad (7)$$

where,  $u$ ,  $v$  and  $w$  are the velocity (m/s) components,  $\alpha$  is the thermal diffusivity ( $\text{m}^2/\text{s}$ ),  $\nu$  is the kinematic viscosity ( $\text{m}^2/\text{s}$ ),  $\beta$  is the volume expansion coefficient,  $g$  is the acceleration of gravity ( $\text{m}/\text{s}^2$ ),  $T$  is the temperature ( $^\circ\text{C}$ ),  $\rho$  is the density ( $\text{kg}/\text{m}^3$ ) of fluid in the computational domain, and  $k$  and  $q$  are the thermal conductivity ( $\text{W}/(\text{m}\cdot\text{K})$ ). For speed components, non-slip conditions are valid on all wall boundaries and the boundary conditions are as follows:

- Speed on all wall boundaries,  $u = v = w = 0$  m/s;
- Pressure sphere surface,  $p = 1$  atm;
- Ambient temperature,  $T = T_\infty = 23$   $^\circ\text{C}$ .

In this study, the Monte-Carlo model preferred like similar studies in the literature because of its numerical stability and precision in the results for the calculation of the heat transfer by radiation [5].

For definition of azimuth and inclination angles general range of scanning for azimuth is  $-90^\circ$  to  $90^\circ$  and inclination is  $-10^\circ$  to  $100^\circ$  with consideration of car tilt as  $10^\circ$ .

First of all, thermal analysis is performed at 5-degree intervals and the critical angle ranges are determined according to the temperature values on the parts (Fig 6).

Based on 5 degree results new scanning range is defined and used as input for 2-degree analysis to define precise angle detection (Fig 7).

After the precise angle detection taken from the peaks of 2 degree results, thermal analysis are repeated by taking the environmental ambient temperature at  $80$   $^\circ\text{C}$  in order to simulate the maximum operating conditions.

**Tubus**

Identification of critical angle of solar irradiation

- Full CFD approach
- Identified angle of incident radiation

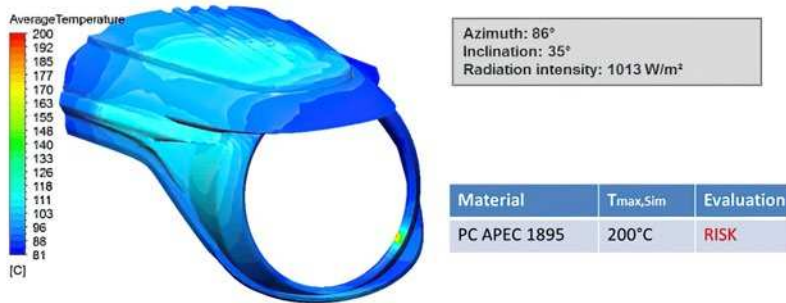


Fig. 8. Tubus thermal analysis results

**HID Frame**

Identification of critical angle of solar irradiation

- Full CFD approach
- Identified angle of incident radiation ( $\Theta_{ambient} = 80^\circ\text{C}$ )

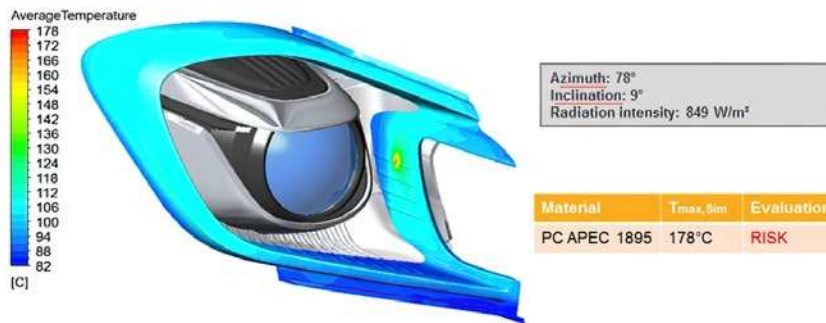


Fig. 9. HID frame thermal analysis results

**Black Seperator**

Identification of critical angle of solar irradiation

- Full CFD approach
- Identified angle of incident radiation



Fig. 10. Black separator thermal analysis results

**3. RESULTS**

**3.1. Numerical Study**

Latest thermal simulations were performed on precised angles which are taken from 2-degree analysis results. Analysis results for all related components given at Table 1.

For tubus part (Fig 8) which is coming from a project, critical angle is defined as azimuth 86° and

inclination 35°. Thermal simulation is performed for this precise angle with defined radiation intensity and ambient temperature taken as 80 °C. Vicat softening temperature of the different grades of polycarbonate taken into consideration for risk evaluation [6]. Maximum temperature on tubus was calculated as 200 °C.

For HID frame (Fig 9) critical angle is defined as azimuth 78° and inclination 9°. Maximum temperature on tubus was reached to 178 °C.

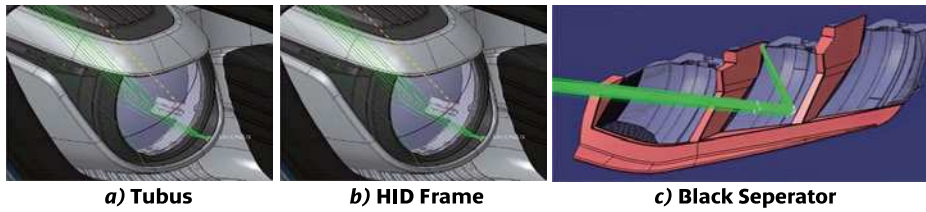


Fig. 11. Hotspot analysis results tubus (a), HID frame (b), black separator (c)

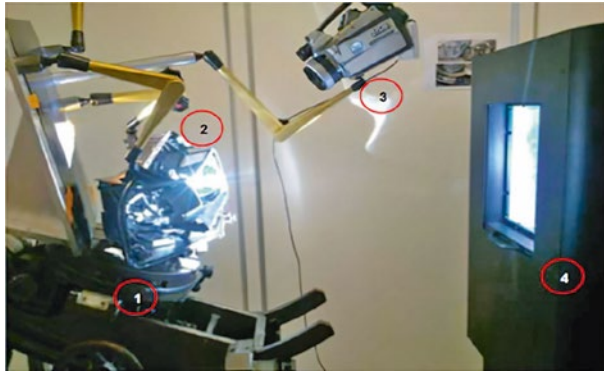


Fig. 12. Front lighting test mechanism (goniometer (1), front lighting (2), thermal camera (3), solar load device (4))

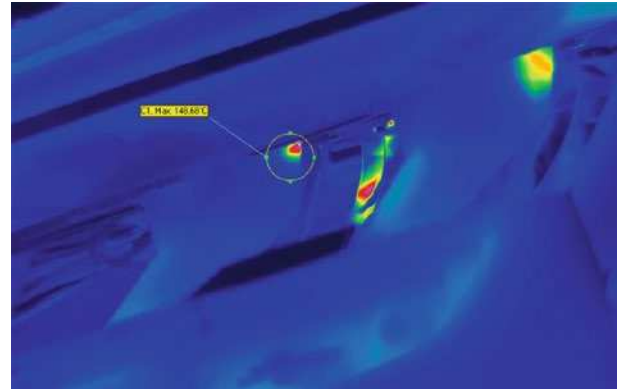


Fig. 13. Thermal camera results of black separator

For black separator (Fig 10) critical angle is defined as azimuth  $-14^\circ$  and inclination  $15^\circ$ . Maximum temperature on tubus was calculated as  $190^\circ\text{C}$ .

### 3.2. Optical Study

The optical system is created according to the critical angles found in the result of thermal analysis for the detection of the focusing levels of the solar rays that make up the hotspot. An optical stage is prepared by using the module written by Automotive Lighting Company.

The module lens used in the prepared optical system, peripheral parts (HID frame, tubus, etc.) and the outer lens absolutely must be. A central point is created on the module lens and the axis system is created on this point. This axis system must be exactly the same as the axis of the light source used. By using this axis system, lines are formed according to the critical angles determined later and the axis system is created for the future region of the sun rays. The direction of the destination of

the new axis system formed is determined according to the light source and a previously simulated *solar.dis* file (luminous distribution file, belonging to the module) is inserted into this axis system. The optical stage is simulated on the front of the lighting product. The name of this stage is determined as measure screen. The lights coming from the light sources used and the lighting product in a refracted or reflected way hit this stage, and in this way, it's possible to simulate the illumination on the road [7]. The surfaces that are hotspots in the optical system are taken as mandatory and ray traces analysis is initiated by using at least 1million rays. The places of the hotspots on the measurement screen are detected by the back ray traces analysing from which surfaces the rays coming out of the solar light source by refracting from the module lens. The controls carried out as a result of the optical system established according to the angles found as risky in the results of thermal analysis and the focusing levels have been given in Fig 11.

### 3.3. Test Studies

The analysis of the completed samples validated by the test setup prepared at the critical angles. The front lighting product is placed on the goniometer and exposed to the solar load. The goniometer, which can move horizontally and vertically, is brought to the critical angles determined by the analysis and the solar load at this point is adjusted

Table 1. Critical Angles

Part Description	Critical angles
Tubus	Az.: $86^\circ$ Inc.: $35^\circ$
Black Separator	Az.: $-14^\circ$ Inc.: $15^\circ$
HID Frame	Az.: $78^\circ$ Inc.: $9^\circ$
Cover Panel	Az.: $3^\circ$ Inc.: $69^\circ$

**Table 2. Analysis and Test Results**

Part Description	Critical Angles	Sim. Res. (°C)	Test Res. (°C)	Difference Rate (%)
Tubus	Az.: 86° Inc.: 35°	200	194	3,00
Black Sperator	Az.: -14° Inc.: 15°	190	188	1,05
HID Frame	Az.: 78° Inc.: 9°	178	184	3,37
Cover Panel	Az.: 3° Inc.: 69°	129	131	1,55

from the test device and the measurements are performed on the parts, Fig 12.

In Fig. 13 and Fig. 14 thermal measurement results of black separator and HID frame have been given, respectively. Measurements have been performed with thermal camera at ambient temperature 23 °C. According to the thermal camera measurements on black separator maximum temperature is found as 148,68 °C and on HID frame found as 144,40 °C.

#### 4. DISCUSSION AND EVALUATION

As the tests have been carried out at ambient temperature, the offset values have been added to the test results in order to obtain an ambient temperature of 80 °C depending on the inclination angle determined to be compatible with the analysis results.

In Table 2, the analysis and the test results have been given. The results of the analysis have been compared with the measurements carried out with a thermal camera and the error rates have been ex-

amined. The maximum difference rate has been determined on the HID frame part with 3.37 %. Difference rates resulting from plastic parts warpage, assembly and production tolerances may vary in a negative or positive direction. Therefore, according to the temperature values determined after analysis, a minimum security margin of 10 °C is predicted for the softening temperatures of plastic materials, thus preventing the deviations specified to cause damage on the part.

#### 5. CONCLUSION

The determined rates of difference are within the 5 % range and the correlation of the analysis and test results have been provided. The selected thermoplastic materials have been prevented from being exposed to colour fading, deformation, gas output and burns generated as a result of long-term loads under the maximum solar load to be exposed in the field. In the subsequent studies, the conduct of studies for different raw material colours, the optimization of the analysis inputs and the correlation with the test results are planned.

#### REFERENCES

1. Neonsee, Application Note, The burning glass effect optical hot spot characterization for the automotive industry, 2011, 1.
2. Sivak M, Schoettle B, Flannagan MJ Mercury-free HID lamps: glare and colour rendering. *Light Res Technol*, 2006, Vol. 38, #1, pp. 33–40.
3. Jang S, Shin WS Thermal analysis of LED arrays for automotive head lamp with a novel cooling system. *IEEE Trans Dev Mater Reliab*, 2008, 8, #3, pp. 561–564.

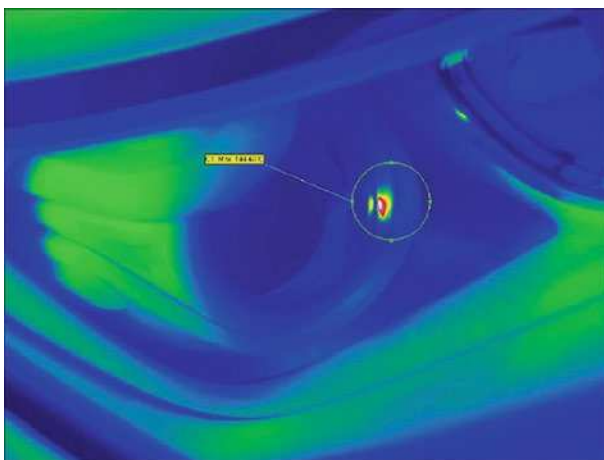


Fig. 14. Thermal camera results of HID frame

4. Kasten, F. and Young, A.T., Revised optical air mass tables and approximation formula. Applied Optics, 1989, #28, pp. 4735–4738.

5. Fischer, P., “Radiative Heat Redistribution and Natural Convection Flow Inside an Automotive Fog Lamp”, Proceedings of the Sixth International Symposium on Automotive Lighting, Darmstadt, Germany, 2001.

6. [https://www.plastics.covestro.com/~media/Product%20Center/PCS/Images/5\\_Library/Product%20brochures/Apec/Apec%20brochure.pdf?la=en&force=1](https://www.plastics.covestro.com/~media/Product%20Center/PCS/Images/5_Library/Product%20brochures/Apec/Apec%20brochure.pdf?la=en&force=1)

7. B. v. Blanckenhagen, Accurate Stray Light Simulations with the Bi- Directional Reflection Distribution Function, ISAL, 2005, p.39.



***Emre Öztürk,***

graduated from Bursa Uludag University, Faculty of Engineering and Architecture, Department of Industrial Engineering in 2008, has got Ms. Degree from Bursa Uludag University, Institute of Science and Technology, Department of Industrial Engineering – Engineering Technology and Management in 2014



***Mehmet Aktaş***

graduated from Eskişehir Osmangazi University, Faculty of Engineering and Architecture, Department of Mechanical Engineering in 2011, has got his Ms. Degree from Eskişehir Osmangazi University, Institute of Science and Technology, Department of Mechanical Engineering – Energy in 2013



***Tunç Şenyüz***

graduated from Canakkale Onsekiz Mart University, Faculty of Sciences and Arts, Department of Physics in 2006, has got his Ms. Degree from Canakkale Onsekiz Mart University, Institute of Science, Department of Space Science and Technologies in –2010, and Doctorate in Canakkale Onsekiz Mart University, Institute of Science, Department of Physics